Efficient Channel Estimation for Cooperative Broadcast in Infrastructure-Based Vehicle Networks

Yizhe Wang†, Shuoling Liu†, Lizhao You†, Yihua Tan◇, Zhaorui Wang§, and Liqun Fu†

†School of Informatics, Xiamen University, China
◇Department of Information Engineering, The Chinese University of Hong Kong, China
§FNii and SSE, The Chinese University of Hong Kong (Shenzhen), China
Corresponding Email: lizhaoyou@xmu.edu.cn

***Abstract*—Cooperative broadcast, allowing simultaneous transmission from multiple roadside units (RSUs), is promising for high-rate information dissemination to on-board units (OBUs) in infrastructure-based vehicle networks. However, the superimposed channel, with multipaths and large frequency spread, makes the traditional 802.11 algorithm that directly estimates the channel ill-suited. Furthermore, due to non-ideal sampling, the superimposed ultimate channel may not exhibit sparsity in practice, degrading the performance of spares channel estimation algorithms. To address these challenges, we present a progressive two-stage channel estimation algorithm that does not rely on the channel sparsity assumption and does not assume the prior knowledge of multipath structure. To further reduce computational complexity, a progressive greedy strategy is adopted, achieving a runtime reduction of over 2.6× compared to the un-optimized two-stage algorithm. Simulation and experimental results show that the proposed two-stage algorithm outperforms the conventional IEEE 802.11 approach in bit error rate (up to 10 dB improvement) and packet error rate (up to 2.5× reduction).**

I. Introduction

Infrastructure-based vehicle networks play a crucial role in enabling autonomous driving [1]. With the assistance of infrastructure such as roadside units (RSUs), common message data can be transmitted to autonomous vehicles, such as traffic condition (e.g., car crash) and point cloud, greatly enhancing safe decision-making. However, achieving high-rate and reliable information dissemination remains a challenge for infrastructure-to-vehicle (I2V) communication [2].

Cooperative broadcast by RSUs is a promising approach for enhancing information dissemination efficiency for I2V communication, and has shown effectiveness in Wi-Fi broadcast [3], [4] and vehicle-to-vehicle (V2V) communication [5], [6]. As shown in Fig. 1(a), neighboring RSUs can simultaneously broadcast the same data (we assume that all RSUs can receive the broadcast data through side-channel links) on the same frequency, extending coverage and boosting reliability through simultaneous transmissions. In contrast, the traditional uncooperative broadcast (i.e., unicast) in Fig. 1(b) allows only one RSU to transmit per time slot to avoid collisions, reducing broadcast throughput and increasing latency.

However, the high-speed mobility in vehicular networks and the multipath channel present challenges for cooperative broadcast. Specifically, the received signal at the vehicle is a superimposed signal from multiple RSUs with multiple paths. Each path is associated with a unique time offset (TO) and frequency offset (FO). This multipath with distinct FOs causes substantial non-linear variation in the frequency-domain channel across subcarriers within each OFDM symbol, making it difficult for the traditional 802.11 channel estimation scheme [7] to remain accurate, as it interpolates the superimposed channel using the received superimposed pilots.

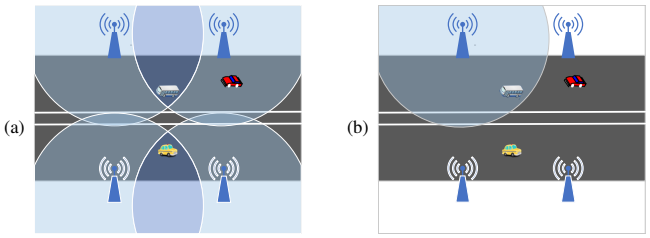

Fig. 1: An example of the broadcast schemes in infrastructure-based vehicle networks: (a) cooperative broadcast with simultaneous RSU transmission; (b) traditional unicast-based uncooperative broadcast with sequential RSU transmission.

There exist several studies that estimate the parameters of each path and then reconstruct the superimposed channel. Specifically, the superimposed channel is formulated as a sum of multiple paths with distinct TOs and FOs. By discreting the TO and FO ranges, the authors in [8] introduced the concept of multi-path sparsity and proposed compressed sensing (CS)-based method. Leveraging channels sparsity, in [9] and [10], the classical orthogonal matching pursuit (OMP) approach has been applied to estimate static and time-varying channels. However, CS-based algorithms that rely on sparsity assumption exhibit inherent limitations. In practice, the superimposed channel may not exhibit ideal sparsity due to factors such as pulse shaping and non-ideal sampling across multipath channels, leading to significant channel leakage and degrading the performance of CS-based estimation.

To address the problem, we use a two stage-based channel estimation approach. The core idea is to first search possible path FOs by partitioning the frequency spreads into finely spaced bins, and then directly derive the time-domain channel taps corresponding to each path. We first construct an input-output model of the superimposed signal, formulating the time- and frequency-domain channel as a sum of multiple paths with distinct TOs and FOs under the mobile channel.

Unlike the static scenario in [4], where all paths associated with the same RSU share the same FO, paths from the same RSU may have different FOs due to velocity differences in our mobile scenario. Moreover, the number of paths in the superimposed signal is unknown, complicating the first-step FO estimation. Even if the path count were known, maximum likelihood estimation becomes infeasible since the number of FO combinations grows exponentially with the number of paths. As a result, the traditional two-stage approach in [4] is unsuitable in scenarios with a large FO search space.

To overcome these challenges, we propose a novel two-stage estimation algorithm (Two-Stage-Prog) that does not rely on the prior knowledge of the multipath structure. It introduces a progressive search scheme, which incrementally searches for the path count, terminating once the residual error falls below a threshold. In addition, to further reduce complexity, we use a greedy selection approach that generates new FO combinations based on the previous optimal combination, reducing the number of combinations from exponential to linear in the number of paths.

Simulation results show that the proposed Two-Stage-Prog algorithm outperforms the CS-based method by 4 dB SNR at a BER of 2×10^{-2}. We also conduct experiments to collect real-world channel and perform trace-driven simulations. Experimental results show that Two-Stage-Prog achieves lower PER compared with CS-based and 802.11 methods (0.3 vs. 0.6 vs. 0.8 at 30 dB) for packet size of 1500-Bytes.

Notations. For clarity, a complete list of the notations used in this paper is provided in Appendix A.

II. System Model

We consider a cooperative broadcast scenario, where U transmitters (i.e., RSUs) simultaneously transmit signals to a receiver (i.e., OBU). The RSUs are coordinated through a master–slave architecture: the master RSU transmits a synchronization frame to align the slave RSUs for simultaneous transmission. Time synchronization is achieved by detecting the frame boundary, while frequency synchronization is performed via FO estimation and phase precoding at the slave RSUs, similar to the uplink OFDMA coordination mechanism in 802.11ax. It is important to note that this synchronization is coarse and does not provide precise phase alignment. Meanwhile, we adopt the standard frame format defined in IEEE 802.11bd [11], with further details provided in Appendix B.

Let $\mathcal{U}$ be a set of transmitters, and $U = |\mathcal{U}|$. Each channel between transmitter $u \in \mathcal{U}$ and the receiver consists of N_u multipath components. For the p-th path, let α_u^p, Δt_u^p and Δf_u^p denote the amplitude, TO and FO, respectively. The TO is defined with respect to the demodulation start position. The FO includes both the residual carrier frequency offset δ_u^p and the Doppler shift ν_u^p, i.e., $\Delta f_u^p = \delta_u^p + \nu_u^p$. The Doppler shift is denoted by $\nu_u^p = \frac{v_u^p}{c} f_c$, where v_u^p is the relative velocity of the p-th path, f_c is the carrier frequency and c is the speed of electromagnetic wave. Because different paths generally arrive with different incidence angles, their relative velocities differ, resulting in distinct FOs across multipath components.

The baseband equivalent channel impulse response from transmitter u to the receiver [12] is given by

$$\bar{h}_u(t,\tau) = \sum_{p=0}^{N_u-1} \bar{\alpha}_u^p \delta(\tau - \Delta t_u^p) \cdot \mathrm{e}^{j2\pi \Delta f_u^p t}, \tag{1}$$

where $\delta(t)$ is the Dirac delta function. The symbol $\bar{\alpha}_u^p$ is the complex channel gain and $\mathrm{e}^{j2\pi\Delta f_u^p t}$ can be treated as an additional phase caused by FO.

Considering the OFDM system in the cooperative broadcast scenario. Denote the bandwidth (or sampling frequency) by W, the number of subcarriers used in OFDM by N, and the OFDM symbol duration by T. The subcarriers spacing is $\frac{W}{N} = \frac{1}{T}$. Let $x(t)$ denote the transmitted time domain OFDM signal in one symbol duration. After the signal $x(t)$ from transmitters in set $\mathcal{U}$ interacts with the channels, the superimposed signal can be expressed as

$$y(t) = \sum_{u\in\mathcal{U}} \sum_{p=0}^{N_u-1} \bar{\alpha}_u^p e^{j2\pi\Delta f_u^p t} x(t - \Delta t_u^p) + w, \tag{2}$$

where w is zero-mean additive white Gaussian noise (AWGN).

Correspondingly, let $\mathbf{F}$ denote an unitary matrix that is formed by cyclically shifting the DFT results by $\frac{N}{2}$ points. In this way, for a sequence of time-domain samples $\mathbf{x} \in \mathbb{C}^N$, the vector $\mathbf{X} = \mathbf{F}\mathbf{x}$ is the output of the shifted DFT. For a Fourier transform pair $x(t) \leftrightarrow X(f)$, we have $x(t - \Delta t) \leftrightarrow X(f)e^{-j2\pi f \Delta t}$. Then, the received frequency-domain signal in (2) can be expressed as

$$\mathbf{Y} = \sum_{u\in\mathcal{U}} \sum_{p=0}^{N_u-1} \bar{\alpha}_u^p \mathbf{\Phi}_{\Delta t_u^p} \mathbf{F} \mathbf{\Phi}_{\Delta f_u^p} \mathbf{x} + \mathbf{w}, \tag{3}$$

where

$$\mathbf{\Phi}_{\Delta t_u^p} = diag(e^{-\frac{j2\pi\Delta t_u^p}{T}\cdot(-\frac{N}{2})}, \ldots, e^{-\frac{j2\pi\Delta t_u^p}{T}\cdot(\frac{N}{2}-1)}), \tag{4}$$

and

$$\mathbf{\Phi}_{\Delta f_u^p} = diag(e^{\frac{j2\pi\Delta f_u^p}{W}\cdot 0}, \ldots, e^{\frac{j2\pi\Delta f_u^p}{W}\cdot(N-1)}), \tag{5}$$

According to $\mathbf{X} = \mathbf{F}\mathbf{x}$, the received signal can be further rewritten as

$$\mathbf{Y} = \sum_{u\in\mathcal{U}} \sum_{p=0}^{N_u-1} \bar{\alpha}_u^p \mathbf{\Phi}_{\Delta t_u^p} \mathbf{F} \mathbf{\Phi}_{\Delta f_u^p} \mathbf{F}^{-1} \mathbf{X} + \mathbf{W}. \tag{6}$$

We assume that the common carrier frequency offset (CFO) across all RSUs is compensated, making inter-carrier interference (ICI) negligible. However, residual frequency offsets (FOs) still remain. We further assume that the channel variation induced by these FOs within a single OFDM symbol is negligible, while the associated phase rotation evolves across symbols. Consider a packet composed of multiple OFDM symbols, each containing an N-point data symbol preceded by a cyclic prefix (CP) of length D. Let $X_{n,k} \in \mathbb{C}$ denote the signal transmitted on the k-th subcarrier of the n-th OFDM symbol, and $Y_{n,k} \in \mathbb{C}$ denote the corresponding received signal. Let c_n denote the sample index of the first sample of the n-th OFDM symbol in the received packet, i.e., $c_n = (n-1)(N+D) + D + 1$. Then the received signal at the k-th subcarrier of the n-th OFDM symbol is described by

$$Y_{n,k} \approx \sum_{u\in\mathcal{U}} \sum_{p=0}^{N_u-1} \bar{\alpha}_u^p \beta_{k,\Delta t_u^p} \phi_{n,\Delta f_u^p} X_{n,k} + W_{n,k}, \tag{7}$$

where $\phi_{n,\Delta f_u^p} = e^{\frac{j2\pi\Delta f_u^p}{W}\cdot(c_n + \frac{N-1}{2})}$ and $\beta_{k,\Delta t_u^p} = e^{-\frac{j2\pi k\Delta t_u^p}{T}}$.

Inefficiency of Current Methods: The channel estimation method proposed for single-user systems [7] relies on linear interpolation of pilots within each symbol. However, this approach is ineffective in the cooperative broadcast scenario. As shown in Eqn. 7, the received signal is a superposition of transmitted signals, each experiencing multiple paths with different delays and frequency shifts. In particular, each RSU's

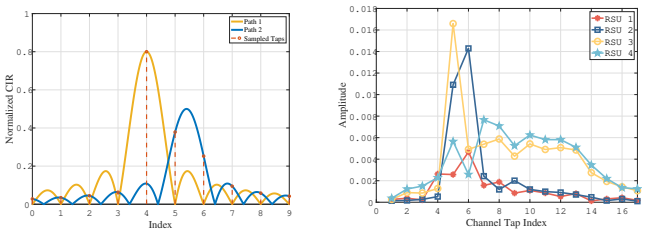

(a) (b)

Fig. 2: Simulation and experimental sampled channel taps in vehicle environment. (a) An example of normalized amplitude of two-path channels; (b) Typical sampled channel taps for a point-to-point OFDM system.

channel varies across symbols, with a linear phase term changing at rate Δf_u^p. Since different RSUs have different rates, the resulting superimposed phase drifts across subcarriers become not-linear. A similar effect occurs for the amplitude, as signals from multiple RSUs can combine constructively or destructively depending on their relative phases.

Another approach is to discretize the delay and frequency domains into two-dimensional grids (e.g., with $\mathcal{M}$ grid points) and assume channel sparsity (i.e., P is much smaller than $\mathcal{M}$) [8]. However, the sparsity assumption does not always valid in practice due to signal leakage introduced by pulse shaping and non-ideal sampling. For instance, Fig. 2(a) illustrates the normalized amplitudes of two propagation paths modulated with a sinc pulse, where the time indices correspond to integer multiples of the sampling interval. Notably, the delays of the propagation paths are not integer multiples of the sampling interval, leading to inter-channel interference. Furthermore, Fig. 2(b) depicts the sampled channel taps obtained from a vehicular experiment (detailed in Section IV-B), where four RSUs sequentially transmit signals to an OBU. It can be seen that the channel leakage around distinct peaks is non-negligible, leading to inter-channel interference, which is consistent with the simulation results. These observations indicate that the sparsity assumption is unsuitable in such cases. To address these challenges, we introduce a new two-stage channel estimation algorithm in the following.

III. Progressive Two-Stage Channel Estimation

A. Overview

In mobile scenarios, the paths associated with the same RSU may experience different Doppler shifts due to relative velocity differences. Without loss of generality, we assume that all paths from different transmitters have different TOs and FOs. Otherwise, paths that have almost the same TOs can be merged during the sampling process. Let $P = \sum_{u\in\mathcal{U}} N_u$ denote the overall number of identifiable paths. Then, the received signal in (7) can be expressed as

$$Y_{n,k} = X_{n,k} \sum_{l=0}^{D-1} \beta_{k,l} \sum_{p=0}^{P-1} \bar{\alpha}_p^l \phi_{n,\Delta f^p} + W_{n,k} \tag{8}$$

where $\beta_{k,l} = e^{-j\frac{2\pi k \Delta t^l}{T}}$ represents the phase shift induced by the l-th delay tap and $\bar{\alpha}_p^l$ denotes the corresponding time-domain channel coefficient. Here, D is the CP length, and the maximum TO is assumed to be within D samples.

We aim to estimate the FO Δf^p and the time-domain channel $\bar{\alpha}_p^l$. To this end, denote the received signal in the n-th symbol as

$$\mathbf{Y}_n = \left[Y_{n,s1}, Y_{n,s2}, \ldots, Y_{n,s_Q}\right], \tag{9}$$

where $\{s_1, s_2, \ldots, s_Q\}$ denote the set of the indices of chosen subcarriers. Let $\mathbf{A}_n \in \mathbb{C}^{Q\times D}$ denote the combination of the transmitted signal and the phase offset induced by TO, i.e.,

$$\mathbf{A}_n = \begin{bmatrix} X_{n,s_1} & \cdots & 0 \\ \vdots & \ddots & \vdots \\ 0 & \cdots & X_{n,s_Q} \end{bmatrix} \begin{bmatrix} \beta_{s_1,0} & \beta_{s_1,1} & \cdots & \beta_{s_1,D-1} \\ \vdots & \vdots & \ddots & \vdots \\ \beta_{s_Q,0} & \beta_{s_Q,1} & \cdots & \beta_{s_Q,D-1} \end{bmatrix}.$$

Let $\mathbf{H}_{\text{time}} \in \mathbb{C}^{D\times P}$ denote time-domain channel matrix, which is given by

$$\mathbf{H}_{\text{time}} = \begin{bmatrix} \bar{\alpha}_0^0 & \cdots & \bar{\alpha}_0^{P-1} \\ \vdots & \ddots & \vdots \\ \bar{\alpha}_{D-1}^0 & \cdots & \bar{\alpha}_{D-1}^{P-1} \end{bmatrix}. \tag{10}$$

Then the received signal at the n-th symbol can be expressed as

$$\mathbf{Y}_n \approx \mathbf{A}_n \mathbf{H}_{\text{time}} \boldsymbol{\phi}_n + \mathbf{W}_n, \tag{11}$$

where $\boldsymbol{\phi}_n = [\phi_{n,\Delta f^0}, \phi_{n,\Delta f^1}, \cdots, \phi_{n,\Delta f^{P-1}}]^T \in \mathbb{C}^{P\times 1}$ is the FO-induced phase vector.

Therefore, during channel estimation, pilot subcarriers and preambles are employed to estimate $\boldsymbol{\phi}_n$ and $\mathbf{H}_{time}$, respectively. Channel equalization can be performed using a frequency-domain least squares (LS) estimator. In the following, we present the proposed channel estimation method.

B. Two-Stage CE: Handling Unknown Path Number

Let Δf_{max} denote the maximal frequency-shifts of the channel, respectively. Hence the frequency shifts are within $[-\Delta f_{max}, \Delta f_{max}]$. For discrete representation, the frequency is divided into M grids. The grid resolutions of frequency is $\epsilon_f = \frac{2\Delta f_{max}}{M}$. Then the the m-th frequency shifts is given by $\Delta f_m = -\Delta f_{max} + \epsilon_f \cdot m$, where $m = 0, 1, \ldots, M-1$.

Stage I: We apply pilot subcarriers (i.e., $|Q| = 4$) over some data symbols to estimate frequency offsets. Let $\mathcal{I} = \{n_1, n_2, \ldots, n_{|\mathcal{I}|}\}$ denote the set of the indices of used data symbols. Let $\boldsymbol{Y}_{\text{I}}$ denote $\left[\boldsymbol{Y}_{n_1}, \boldsymbol{Y}_{n_2}, \ldots, \boldsymbol{Y}_{n_{|\mathcal{I}|}}\right] \in \mathbb{C}^{Q\times|\mathcal{I}|}$ and $\boldsymbol{\phi}_{\text{I}}$ denote $\left[\boldsymbol{\phi}_{n_1}, \ldots, \boldsymbol{\phi}_{n_{|\mathcal{I}|}}\right] \in \mathbb{C}^{P\times|\mathcal{I}|}$. Then

$$\mathbf{Y}_{\text{I}} \approx \bar{\mathbf{A}}_{\text{I}} \boldsymbol{\phi}_{\text{I}} + \mathbf{W}, \tag{12}$$

where $\bar{\mathbf{A}}_{\text{I}} = \mathbf{A}_{\text{I}} \mathbf{H}_{\text{time}}$. Since the pilots for all data symbols are the same, we have $\mathbf{A}_{\text{I}} = \mathbf{A}_n \in \mathbb{C}^{Q\times D}$ for all $n \in \mathcal{N}$. At the i-th iteration, let $\Delta f_i^p \in \{\Delta f_0, \Delta f_1, ..., \Delta f_{M-1}\}$ denote the value being searched by path p and let $\boldsymbol{\Delta f}_i = \left[\Delta f_i^0, \Delta f_i^1, ..., \Delta f_i^{P-1}\right], i = 1, 2, ..., E$ denote the value being searched by all RSUs, where E denotes the number of combinations of the searched vector.

Our aim is to find the most matched $\boldsymbol{\Delta f}_i$ against $\mathbf{Y}_{\text{I}}$. Let $\boldsymbol{\phi}_{\text{I}}^+(\cdot)$ denote the pseudo-inverse, and $\boldsymbol{\phi}_{\text{I}}^*(\cdot)$ denote the conjugate transpose. We first compute $\hat{\mathbf{A}}_{\text{I}}$ as $\mathbf{Y}_{\text{I}} \boldsymbol{\phi}_{\text{I}}^+(\boldsymbol{\Delta f}_i)$, where $\boldsymbol{\phi}_{\text{I}}^+(\boldsymbol{\Delta f}_i) = \boldsymbol{\phi}_{\text{I}}^*(\boldsymbol{\Delta f}_i) \left(\boldsymbol{\phi}_{\text{I}}(\boldsymbol{\Delta f}_i) \boldsymbol{\phi}_{\text{I}}^*(\boldsymbol{\Delta f}_i)\right)^{-1}$, and then reconstruct the estimated signal as $\hat{\mathbf{Y}}_{\text{I}} = \hat{\mathbf{A}}_{\text{I}} \boldsymbol{\phi}_{\text{I}}(\boldsymbol{\Delta f}_i)$. Then, the matching error of the i-th element is given by

$$e_i = ||\mathbf{Y}_{\text{I}} - \mathbf{Y}_{\text{I}} \boldsymbol{\phi}_{\text{I}}^+(\boldsymbol{\Delta f}_i) \boldsymbol{\phi}_{\text{I}}(\boldsymbol{\Delta f}_i)||_F. \tag{13}$$

Then, the estimated FO set is given by

$$\boldsymbol{\Delta}\hat{\mathbf{f}} = \boldsymbol{\Delta}\mathbf{f}_{i^*},\ i^* = \min_i e_i. \tag{14}$$

However, the total number of paths P experienced by superimposed signals from different RSUs is unknown in practice. As a consequence, the term $\boldsymbol{\Delta}\mathbf{f}_i$ cannot be determined a priori. One possible approach is to pre-generate the FO search set assuming all possible number of paths, and pre-compute $\boldsymbol{\phi}_{\mathrm{I}}(\cdot)$ and its pseudo-inverse for each element in the set, similar to the method proposed in [4]. Nevertheless, the number of the pre-generated vectors grows exponentially as the number of FOs, especially when a single RSU experiences multiple FOs. This results in two challenges: 1) the pre-generated vectors consume a large amount of memory; 2) searching for the optimal FO pair in (14) is time-consuming.

To address these issues, we present a *progressive* search method. Let $\mathcal{P}$ be the number of paths in the received signal, and $\mathbb{S}^{\mathcal{P}}$ be the search set of the FOs. We search from $\mathcal{P} = 1$. For each $\mathcal{P}$, we compute the matching error $\mathbf{e}^{\mathcal{P}}$ on the set $\mathbb{S}^{\mathcal{P}}$ according to (13), and the normalized reduced residual error as

$$\xi^P = \frac{|\mathbf{e}^{\mathcal{P}} - \mathbf{e}^{\mathcal{P}-1}|}{\mathbf{e}^{\mathcal{P}-1}}. \tag{15}$$

If the residual error is less than the pre-defined threshold η, the estimated FOs are assumed to be close to the true values, and the search is terminated. In this way, our method works when the prior number of paths is unknown in practice.

Meanwhile, instead of completely enumerating all combinations for each $\mathcal{P}$, we adopt a *greedy* approach to construct $\mathbb{S}^{\mathcal{P}+1}$ based on the found optimal FO pair $\boldsymbol{\Delta}\mathbf{f}$ on $\mathbb{S}^{\mathcal{P}}$. In particular, we assume that the FOs of the first $\mathcal{P}$ paths remain the same, and only allow the new path to have the value in the quantized FO range. In this way, this method does not require the pre-generated matrix, and significantly reduces the memory usage and the computation complexity. In conventional two-stage algorithm, the total number of required searches is $\mathcal{O}\left(\sum_{\mathcal{P}=1}^{P} M^{\mathcal{P}}\right)$, which grows exponentially with the number of paths. In contrast, the proposed algorithm searches the paths sequentially, reducing the overall search complexity to $\mathcal{O}(MP)$ and lowering the computational burden from exponential to linear-product order.

Stage II: Preambles are utilized to estimate the time-domain channel (i.e., $|Q| = 52$). Given preambles are repeatedly inserted into the frame in IEEE 802.11bd, we can choose several preamble symbols for estimation.

Denote $\mathcal{II} = \{n_1, n_2, \ldots, n_{|\mathrm{II}|}\}$ the set of the indices of used data symbols. Then

$$\mathbf{Y}_{\mathrm{II}} \approx \mathbf{A}_{\mathrm{II}}\mathbf{H}_{\mathrm{time}}\boldsymbol{\phi}_{\mathrm{II}} + \mathbf{W}, \tag{16}$$

where $\mathbf{A}_{\mathrm{II}} = \mathbf{A}_n \in \mathbb{C}^{Q\times D}, n \in \mathcal{N}$. The estimated time-domain channel is expressed as

$$\hat{\mathbf{H}}_{time} = \mathbf{A}_{\mathrm{II}}^{+}\mathbf{Y}_{\mathrm{II}}\boldsymbol{\phi}_{\mathrm{II}}^{+}. \tag{17}$$

With the estimated FOs $\boldsymbol{\Delta}\hat{\mathbf{f}}$ and the time-domain channel $\hat{\mathbf{H}}_{time}$, the frequency-domain channels in each OFDM data symbol can be recovered by (11). The overall progressive two-stage channel estimation algorithm is summarized in Algorithm 1.

Algorithm 1 Two-Stage-Prog Channel Estimation

```
Input received signals Y_I in (12) and Y_II in (16);
Initialization: P = 0; Δf = [];
while ξ^P > η do
    P = P + 1
    S^P = ∅                                   ▷ the search set
    for m = 1, 2, ..., M do
        Δf' = Δf ∪ Δf_m                       ▷ the search element
        S^(P) ← S^(P) ∪ Δf'                   ▷ add the element to the set
    end for
    Compute the matching error e^P according to (13)
    Get the optimal FO vector Δf on the set S^P according to (14)
    Compute the residual error ξ^P according to (15)
end while
Get the corresponding φ_II according to (16)
Compute time-domain channel Ĥ_time according to (17).
```

IV. Evaluation

A. Simulation Setup and Results

1) Setup: We use the IEEE 802.11bd frame format, where training sequences (midambles) are allowed to be inserted periodically. QPSK modulation and the rate 1/2 LDPC codes are used. Each LDPC block has 1944 bits. We consider the point cloud broadcast application with high data rate requirement. Each packet has 300 data symbols (around 1500 Bytes) and midambles are inserted periodically every 16 symbols. The central frequency is 5.8GHz and the bandwidth is 10MHz.

We adopt the IEEE 802.11 multi-path channel model with exponential power decay [13]. The root mean square delay spread is set to 100ns. In addition to the channel, we also add random TOs, CFOs, and Doppler frequency shifts. The maximal TO is set to 10 samples, less than the CP length (i.e., 16 samples) to tolerate delay spread. CFOs are generated within the range [-250Hz, 250Hz]. The moving speed is slower than 72km/h (∼45mph) [1]. The maximal Doppler shift is around 393Hz. Each point in the results is obtained by averaging over 10000 randomly generated channels and packets. Signal-to-noise ratio (SNR) is defined as the power of the superimposed signal versus that of the noise signal.

The proposed low-complexity progressive two-stage algorithm is referred to as *Two-Stage-Prog*. For comparison, we consider the following channel estimation algorithms:

- Matching Pursuit: a CS-based method that discretizes TOs and FOs into grids according to the model in (7), and constructs a dictionary matrix for sparse recovery [8];
- 802.11: a modified algorithm based on [7], which assumes the phase drift caused by FOs is approximately linear across subcarriers. The channel is interpolated using pilots and periodically updated using midambles.
- Optimal: the optimal algorithm assuming known time-domain channels and FOs.

We use the following metrics for comparison: normalized mean square error (NMSE) of the estimated channel and BER before channel decoding.

[1]The algorithm also performs reliably at higher speeds (80–120 km/h). Detailed results as shown in Appendix C.

TABLE I: Running time (s) of two-stage algorithms.

Algorithm	4 paths	5 paths	6 paths
Two-Stage	0.652953	8.91879	–
Two-Stage-Prog	0.182918	0.238498	0.353274

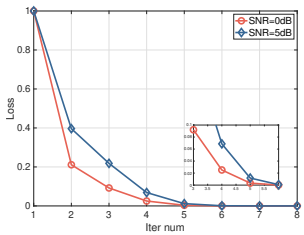

Fig. 3: Reduced error results of Two-Stage-Prog.

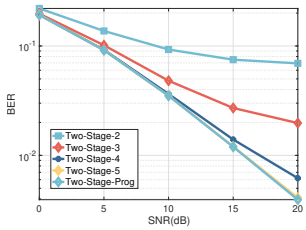

Fig. 4: BER results of two-stage algorithms.

2) Results: To demonstrate the efficacy of the Two-Stage-Prog algorithm, we first present the normalized reduced error result during the progressive search phase, depicted in Fig. 3. In the simulation, each RSU has two paths, and there are four RSUs. The threshold η is set to 0.03. As the search stage progresses, the residual error gradually flattens out, and the search stops at the fifth round for both SNRs, meaning that the algorithm can terminate.

Fig. 4 shows the BER results for the traditional two-stage algorithms and the Two-Stage-Prog algorithm. In the traditional two-stage algorithms, the number of paths is set to 2, 3, 4, and 5, respectively. The Two-Stage-Prog algorithm outperforms the fixed number version other than 5, and approach the Two-Stage-5 algorithm, meaning that the greedy search strategy introduces negligible performance loss. Meanwhile, the running time of Two-Stage-Prog is significantly reduced by more than 2.6× (i.e., 0.18s vs 0.65s) compared with the complete enumeration approach as shown in Table I. Furthermore, as the search range increases, the running time of the proposed new two-stage algorithm increases linearly. However, the traditional two-stage algorithm cannot operate when the number of paths exceeds 5 due to memory limitations caused by the pre-computation and storage.

Fig. 5 shows the NMSE and BER results for the concurrent transmission with four RSUs. The proposed two algorithms show better performance than the 802.11 algorithm. Specifically, at a BER of 2×10^{-2}, the proposed two-stage algorithm is 10dB better than the 802.11 algorithm. This is because the superimposed signal experienced non-linear phase rotation and the 802.11 algorithm become ineffective. Furthermore, although the MP algorithm outperforms 802.11, its performance shows an error floor at the high SNR regime. The proposed two-stage algorithm achieves 4dB SNR gain than the MP algorithm at BER 2×10^{-2}. This improvement is attributed to the fact that the proposed algorithm does not rely on prior knowledge of the multipath structure. In contrast, the MP algorithm is constrained by the channel sparsity assumption and is further affected by the highly correlated sensing matrix.

B. Experimental Setup and Results

We adopt the trace-driven approach to evaluate the physical-layer decoding performance. We conduct experiments using two USRPs, one as an RSU on the roadside and the other as

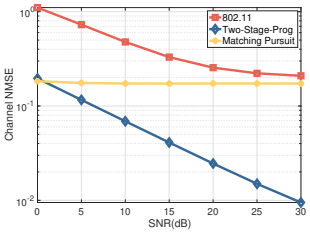

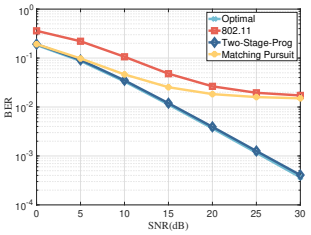

Fig. 5: Simulation results of different algorithms (four RSUs).

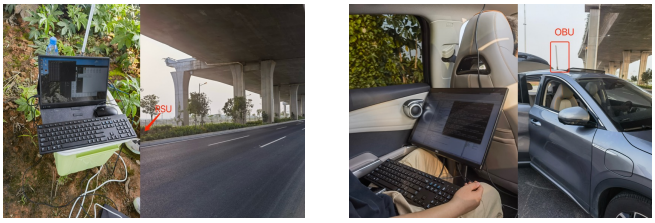

(a) (b)

Fig. 6: Experiment environment: (a) RSU; (b) OBU.

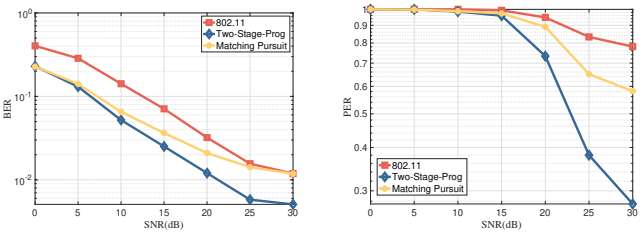

Fig. 7: Experimental results of diff. algorithms (four RSUs).

an OBU on the car with moving speed around 30km/h. Hence, the collected signals experienced Doppler shifts. The outdoor experiment environment is shown in Fig. 6. We first record the baseband signals of the point-to-point communication, and then manually add them with various TOs and FOs to emulate different reception situations. The TO and FO range is set as the same in simulations. Each time, we randomly choose four packet traces to generate the superimposed signal.

Fig. 7 shows the BER and PER results assuming four concurrent transmitters. The experiment results are consistent with the simulation results. The proposed algorithm outperform the MP and 802.11 algorithms in PER (e.g., 0.3 vs. 0.6 vs. 0.8 at SNR=30dB). Specifically, the traditional 802.11 algorithm has a high PER for most SNRs. The MP algorithm exhibits an error floor at the high SNR, while the Two-Stage-Prog algorithm has a much lower PER.

V. Conclusion

This paper presents a progressive two-stage channel estimation algorithm to enable efficient cooperative broadcast in infrastructure-based vehicular networks, addressing challenges from multipaths and large frequency spread in the superimposed signal. Simulation and experimental results show that the algorithm significantly outperforms both CS-based and the conventional IEEE 802.11 methods. In future work, we plan to conduct theoretical analyses, such as deriving the Cramér–Rao bound, to characterize the algorithm's performance limits.

REFERENCES

[1] S. Jung, J. Kim, M. Levorato, C. Cordeiro, and J.-H. Kim, "Infrastructure-assisted on-driving experience sharing for millimeter-wave connected vehicles," *IEEE Transactions on Vehicular Technology*, vol. 70, no. 8, pp. 7307–7321, 2021.

[2] S. Shi, N. Ling, Z. Jiang, X. Huang, Y. He, X. Zhao, B. Yang, C. Bian, J. Xia, Z. Yan *et al.*, "Soar: Design and deployment of a smart roadside infrastructure system for autonomous driving," in *ACM MobiCom*, 2024, pp. 139–154.

[3] H. Qiu, K. Psounis, G. Caire, K. M. Chugg, and K. Wang, "High-rate wifi broadcasting in crowded scenarios via lightweight coordination of multiple access points," in *ACM MobiHoc*, 2016, pp. 301–310.

[4] L. You, S. Liu, W. Xie, Z. Wang, Y. Tan, and S. C. Liew, "Improving cooperative Wi-Fi broadcast with fine-grained channel estimation," in *IEEE/ACM IWQoS*, 2024, pp. 1–10.

[5] T. Das, L. Chen, R. Kundu, A. Bakshi, P. Sinha, K. Srinivasan, G. Bansal, and T. Shimizu, "CoReCast: Collision resilient broadcasting in vehicular networks," in *ACM MobiSys*, 2018, pp. 217–229.

[6] H. Zeng, H. Pirayesh, P. K. Sangdeh, and A. Quadri, "VehCom: Delay-guaranteed message broadcast for large-scale vehicular networks," *IEEE Trans. Wireless Commun.*, vol. 20, no. 6, pp. 3883–3896, 2021.

[7] B. Bloessl, M. Segata, C. Sommer, and F. Dressler, "An IEEE 802.11 a/g/p OFDM receiver for GNU radio," in *ACM SRIF*, 2013, pp. 9–16.

[8] W. U. Bajwa, J. Haupt, A. M. Sayeed, and R. Nowak, "Compressed channel sensing: A new approach to estimating sparse multipath channels," *Proceedings of the IEEE*, vol. 98, no. 6, pp. 1058–1076, 2010.

[9] A. Alkhateeb, O. El Ayach, G. Leus, and R. W. Heath, "Channel estimation and hybrid precoding for millimeter wave cellular systems," *IEEE J. Sel. Top. Sign. Proces.*, vol. 8, no. 5, pp. 831–846, 2014.

[10] Q. Qin, L. Gui, P. Cheng, and B. Gong, "Time-varying channel estimation for millimeter wave multiuser mimo systems," *IEEE Trans. Veh. Technol.*, vol. 67, no. 10, pp. 9435–9448, 2018.

[11] F. Berens, S. Sand, V. Martinez, S. Rührup, and R. Rui, "Next generation v2x-ieee 802.11 bd as fully backward compatible evolution of ieee 802.11 p," *Car 2 Car Communication Consortium*, 2023.

[12] D. Tse and P. Viswanath, *Fundamentals of wireless communication*. Cambridge university press, 2005.

[13] Y. S. Cho, J. Kim, W. Y. Yang, and C. G. Kang, *MIMO-OFDM wireless communications with MATLAB*. John Wiley & Sons, 2010.

APPENDIX A
SUMMARY OF SYSTEM AND ALGORITHM PARAMETERS

For ease of reference, the major symbols used in this paper are summarized in Table II.

TABLE II: Summary of System and Algorithm Parameters

Symbol	Description
$\mathcal{U}$, U	Set and number of transmitters (RSUs)
N_u	Number of channel paths from RSU u to the OBU
P	Total number of paths in the superimposed channel
$\bar{\alpha}_u^p$	Complex gain of the p-th path from RSU u
Δt_u^p	Time offset (TO) of the p-th path from RSU u
Δf_u^p	Frequency offset (FO) of the p-th path from RSU u
δ_u^p	Residual carrier frequency offset of the p-th path
ν_u^p	Doppler shift of the p-th path from RSU u
v_u^p	Relative velocity associated with the p-th path
f_c	Carrier frequency
c	Speed of electromagnetic wave
W	System bandwidth (sampling frequency)
N	Number of OFDM subcarriers
D	Cyclic-prefix (CP) length in samples
T	OFDM symbol duration (without CP)
$x(t)$	Transmitted time-domain OFDM signal
$y(t)$	Superimposed received time-domain signal
w	Additive white Gaussian noise (AWGN) in time domain
$X_{n,k}$	Transmitted symbol on subcarrier k of OFDM symbol n
$Y_{n,k}$	Received symbol on subcarrier k of OFDM symbol n
$W_{n,k}$	Frequency-domain AWGN on subcarrier k of symbol n
c_n	Sample index of the first sample of the n-th OFDM symbol
$\phi_{n,\Delta f_u^p}$	Phase rotation factor induced by FO on symbol n
$\beta_{k,\Delta t_u^p}$	Phase rotation factor induced by TO on subcarrier k
$\mathbf{H}_{\text{time}}$	Time-domain channel matrix collecting all path taps
$\mathbf{Y}_n$	Vector of received pilots (selected subcarriers) of symbol n
$\mathbf{A}_n$	Pilot-related matrix combining transmit symbols and TO phase
Q	Number of selected subcarriers
$\Delta f_{\max}$	Maximum absolute FO in the search range
M	Number of frequency-grid points in the FO search
ϵ_f	FO grid resolution
Δf_m	FO value of the m-th frequency grid
$\mathcal{P}$	Assumed number of paths in the current search iteration
$\mathbb{S}^{\mathcal{P}}$	FO search set for $\mathcal{P}$ paths
$\mathbf{\Delta f}$	FO vector (one candidate combination of path FOs)
e_i	Matching error of the i-th FO combination
$\xi^{\mathcal{P}}$	Normalized residual error between $\mathcal{P}$ and $\mathcal{P}-1$
η	Threshold for terminating the progressive FO search

APPENDIX B
FRAME FORMAT

We adopt the standard frame format defined in IEEE 802.11bd [11]. Midambles (preambles) are inserted periodically every 16 OFDM data symbols within a frame to enable channel tracking under high-mobility conditions. Each data symbol contains 64 subcarriers, of which 4 are allocated for pilots. This frame format is consistently used throughout the paper, including both simulations and experiments, and for all algorithms. Fig. 8 illustrates the overall frame format, where a midamble consists of two LTSes, and LTS denotes the long training symbols defined in IEEE 802.11 standards.

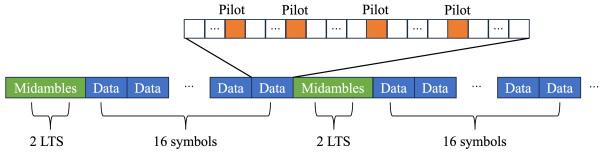

Fig. 8: Frame format of IEEE 802.11bd.

APPENDIX C
SIMULATION RESULTS FOR HIGH-MOBILITY SCENARIOS

We further evaluate the NMSE and BER performance under higher mobility scenarios with speeds of 80 km/h, 100 km/h, and 120 km/h. As shown in Fig. 9, the proposed algorithm consistently achieves the best performance across different speeds. Specifically, the proposed algorithm outperforms the comparative algorithm by at least 4dB at a BER of 10^{-2}. In addition, the performance remains stable as mobility increases, demonstrating the generalization of the propose algorithm under high-mobility conditions.

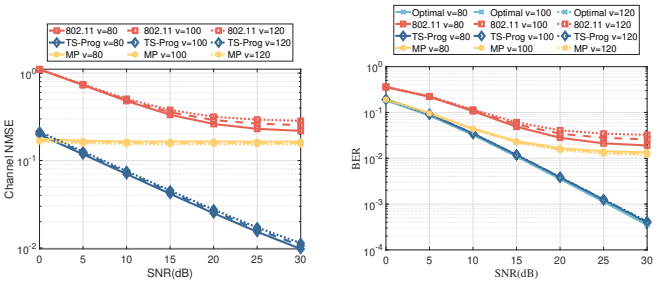

Fig. 9: Simulation results of different velocities (four RSUs).